

Affine Non-negative Collaborative Representation Based Pattern Classification

He-Feng Yin^{*†}, Xiao-Jun Wu^{*†}, Zhen-Hua Feng^{‡§} and Josef Kittler[§]

^{*}School of Artificial Intelligence and Computer Science, Jiangnan University, Wuxi 214122, China

Email: 7141905017@vip.jiangnan.edu.cn, wu_xiaojun@jiangnan.edu.cn

[†]Jiangsu Provincial Engineering Laboratory of Pattern Recognition and Computational Intelligence

Jiangnan University, Wuxi 214122, China

[‡]Department of Computer Science, University of Surrey, Guildford GU2 7XH, UK

Email: z.feng@surrey.ac.uk

[§]Centre for Vision, Speech and Signal Processing, University of Surrey, Guildford GU2 7XH, UK

Email: j.kittler@surrey.ac.uk

Abstract—During the past decade, representation-based classification methods have received considerable attention in pattern recognition. In particular, the recently proposed non-negative representation based classification (NRC) method has been reported to achieve promising results in a wide range of classification tasks. However, NRC has two major drawbacks. First, there is no regularization term in the formulation of NRC, which may result in unstable solution and misclassification. Second, NRC ignores the fact that data usually lies in a union of multiple affine subspaces, rather than linear subspaces in practical applications. To address the above issues, this paper presents an affine non-negative collaborative representation (ANCR) model for pattern classification. To be more specific, ANCR imposes a regularization term on the coding vector. Moreover, ANCR introduces an affine constraint to better represent the data from affine subspaces. The experimental results on several benchmarking datasets demonstrate the merits of the proposed ANCR method. The source code of our ANCR is publicly available at <https://github.com/yinhefeng/ANCR>.

Index Terms—Pattern Classification, Non-negative Representation, Affine Constraint

I. INTRODUCTION

Sparse representation-based classification remains one of the hot research topics in pattern recognition. The most two widely studied approaches include the classical sparse representation based classification (SRC) [1] and collaborative representation based classification (CRC) [2]. SRC directly employs all the training data as the dictionary and sparsely represents a test sample by solving the ℓ_1 -regularized minimization problem. Then the classification task is performed by checking which class yields the least reconstruction error (residual) of the test sample. SRC can achieve impressive classification performance in face recognition even when the test face image is occluded or corrupted. However, it is time consuming to solve the ℓ_1 -regularized minimization problem. To address this issue, Zhang *et al.* [2] advocated the CRC method that uses the ℓ_2 -norm as the regularization term.

Based on the classical SRC and CRC methods, researchers have proposed a variety of improved methods. Liu *et al.* [3] presented a locally linear K nearest neighbor method that combines sparsity, locality, and reconstruction to obtain the

reconstruction coefficients of a test sample. Song *et al.* [4] proposed a progressive SRC algorithm using local discrete cosine transform for face classification. Lai *et al.* [5] developed a class-wise sparse representation method that seeks an optimum representation of the query image by minimizing the class-wise sparsity of the training data. Shao *et al.* [6] proposed a new SRC-based face classification algorithm that exploits dynamic dictionary optimization on an extended dictionary using synthesized faces. Akhtar *et al.* [7] presented a sparsity augmented CRC (SA-CRC) scheme that augments a dense collaborative representation with a sparse representation. Inspired by SA-CRC, Li *et al.* [8] proposed a sparsity augmented weighted CRC approach for image recognition. Deng *et al.* [9] developed a superposed linear representation classifier to cast the recognition problem as one of representing the test image in terms of a superposition of the class centroids and shared intra-class differences. To address the problem of an insufficient number of training samples, Vo *et al.* [10] developed a hierarchical CRC model. Song *et al.* [11] proposed the use of a 3D face model to synthesize faces with pose variations for pose-invariant face recognition. By employing only a subset of known pattern classes to collaboratively represent a test sample, Zheng *et al.* [12] designed a k nearest classes-based CRC scheme. Xie *et al.* [13] presented an elastic-net regularized regression algorithm, which combines shared sparse representation with class specific CRC to represent a test sample. Song *et al.* [14] proposed a half-face based CRC method to perform occlusion invariant face classification. Lan *et al.* [15] proposed a probabilistic CRC method for visual object recognition that includes the characteristics of the training samples of each class as prior knowledge. Gou *et al.* [16] developed a weighted discriminative CRC method that considers the competitive representation of each class and enhances the inter-class discrimination.

Xu *et al.* [17] pointed out that there exist negative elements in the coefficients obtained by SRC, CRC and their variants, which may result in misclassification of test samples. Motivated by non-negative matrix factorization (NMF) [18], they proposed a non-negative representation based classifier (NRC)

that imposes a non-negative constraint on the coding vector. Extensive experiments on diverse classification tasks demonstrate the superiority of NRC over many existing representation based classification methods, including SRC, CRC and their variants. Nevertheless, NRC has two shortcomings. First, due to the lack of regularization term on the coding vector, NRC may produce unstable solutions. Second, NRC cannot effectively deal with the data drawn from affine subspaces. To alleviate these drawbacks, we propose an affine non-negative collaborative representation (ANCR) model, in which a regularizer on the coding vector and the affine constraint are introduced.

To illustrate the mechanism of ANCR, we conduct an experiment on the USPS dataset. This dataset contains images for digits 0-9. 50 images per class are used to form the training set. The training data matrix composed of the 500 images arranged in the order of $[0, 1, 2, \dots, 9]$, is denoted by $\mathbf{X} = [\mathbf{X}_0, \mathbf{X}_1, \dots, \mathbf{X}_9]$. Consider a test sample from the ninth class (i.e., digit 8). The coding vector and residual obtained by NRC are shown in Fig. 1 (a) and Fig. 1 (b). The coding vector and residual obtained by ANCR are shown in Fig. 1 (c) and Fig. 1 (d). From Fig. 1 (b), we can see that the eighth class has the least residual, i.e., the test sample is wrongly recognized as digit 7. Meanwhile, it can be seen in Fig. 1 (a) that the eighth class has dominant coefficients. From Fig. 1 (d), we note that the ninth class results in the minimum residual, i.e., the test sample is correctly recognized as digit 8. When we look more closely at the coding vectors of NRC and ANCR for the eighth class (indices 351-400), the number of nonzero entries are 7 and 14, respectively. In contrast, for the ninth class (indices 401-450), the number of nonzero entries of NRC and ANCR are 16 and 41, respectively. By introducing the coding vector regularizer and affine constraint into NRC, more coefficients are concentrated on the correct class, resulting in improved performance.

The main contributions of the paper are as follows,

- We propose an affine non-negative collaborative representation (ANCR) model by regularizing the coding vector and introducing an affine constraint in the formulation of NRC.
- An optimisation algorithm based on the alternating direction method of multipliers (ADMM) [19] is developed to efficiently solve the optimization problem of ANCR.
- An extensive evaluation of the proposed ANCR method on diverse benchmarking datasets demonstrate that it outperforms conventional representation based classification methods as well as some deep learning based methods.

II. RELATED WORK

In recent years, the non-negative constraint has attracted considerable attention in various research areas. For instance, Vo *et al.* [20] developed a non-negative least square (NNLS) algorithm for face recognition, which represents each new sample as a non-negative linear combination of training samples. Zhuang *et al.* [21] proposed a non-negative low-rank and sparse (NNLRS) graph for semi-supervised learning. Yin *et*

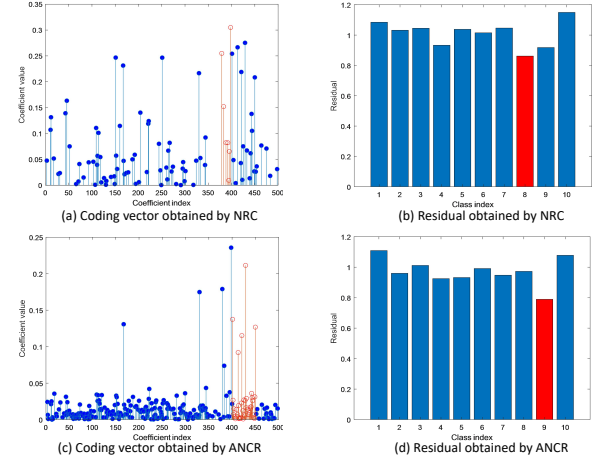


Fig. 1. Coding vectors and residuals obtained by NRC and ANCR: (a) coding vector obtained by NRC; (b) class-specific residual of NRC; (c) coding vector obtained by ANCR; (d) class-specific residual obtained by ANCR. The test sample belongs to the ninth class, i.e., digit 8. We can see that the eighth class yields the least residual for NRC, thus the test sample digit 8 is misclassified as digit 7. In contrast, we note that the ninth class has the minimum residual for our ANCR method, resulting in correct classification result.

al. [22] presented a non-negative sparse hyper-Laplacian regularized LRR model (NSHLRR) for unsupervised and semi-supervised applications. Xu *et al.* [23] developed a unified non-negative subspace representation constrained learning scheme for discriminative correlation filter (DCF) based tracking. Zhang *et al.* [24] presented a normalized non-negative sparse coding (N^3SC) method that enforces both the non-negative constraint and the shift-invariant constraint to the traditional sparse coding criteria. Chen *et al.* [25] designed a non-negative representation based discriminative dictionary learning algorithm (NRDL) for face classification. Xu *et al.* [26] proposed a scaled simplex representation (SSR) for subspace clustering. Xu *et al.* [27] designed a jointly non-negative, sparse and collaborative representation (NSCR) for image recognition. Zhao *et al.* [28] developed a Laplacian regularized non-negative representation (LapNR) method for clustering and dimensionality reduction tasks. Inspired by NRC, Yin *et al.* [29] explored a class-specific residual constraint non-negative representation (CRNR) for pattern classification.

The affine constraint has also been widely exploited in clustering and classification tasks. In sparse subspace clustering (SSC), Elhamifar *et al.* [30], [31] introduced the affine constraint to deal with affine subspaces. Xu *et al.* [32] proposed an affine subspace clustering (ASC) algorithm which incorporates the affine constraint into a ridge regression formulation of the sparse representation problem. Dong *et al.* [33] presented a sparse representation based affine subspace clustering method, which employs the non-convex smoothed ℓ_0 -norm to replace the ℓ_0 norm. In locality-constrained linear coding (LLC) [34], the affine constraint is also referred to as the shift-invariant constraint. Motivated by LLC, Wei *et al.* [35] developed a locality-sensitive dictionary learning algorithm for SRC, in which the designed dictionary is capable of preserving the

local data structure. Benuma *et al.* [36] proposed a kernel locality sensitive discriminative sparse representation (K-LSDSR) for face recognition.

III. THE PROPOSED ANCR METHOD

In this section, we first present a mathematical formulation of our ANCR approach. Then we introduce a detailed solution of the learning ANCR problem. Last, we provide an ANCR-based classification method. For the ease of presentation, we introduce the notation used in this paper. Assume that we have n training samples belonging to K classes, and let the training data matrix be denoted by $\mathbf{X} = [\mathbf{X}_1, \mathbf{X}_2, \dots, \mathbf{X}_K] \in \mathbb{R}^{d \times n}$, where \mathbf{X}_i is the data matrix of the i -th class. The i -th class has n_i training samples and $\sum_{i=1}^K n_i = n$ ($i = 1, 2, \dots, K$), d is the dimensionality of the vectorized samples.

A. Formulation of ANCR

To overcome the drawbacks of NRC, we incorporate the elastic-net regularizer [37], i.e., $\lambda_1 \|\mathbf{c}\|_2^2 + \lambda_2 \|\mathbf{c}\|_1$, into the formulation of NRC. The elastic-net regularizer is a combination of the ℓ_1 -norm and ℓ_2 -norm. Therefore, it has the merits of both the lasso and ridge regression methods. We introduce the affine constraint and obtain the following optimization problem,

$$\begin{aligned} \min_{\mathbf{c}} \quad & \|\mathbf{y} - \mathbf{X}\mathbf{c}\|_2^2 + \lambda_1 \|\mathbf{c}\|_2^2 + \lambda_2 \|\mathbf{c}\|_1 \\ \text{s.t. } \quad & \mathbf{c} \geq 0, \mathbf{1}^T \mathbf{c} = 1 \end{aligned} \quad (1)$$

It is worth noting that since $\mathbf{c} \geq 0$ and $\|\mathbf{c}\|_1 = \mathbf{1}^T \mathbf{c} = 1$. By removing the ℓ_1 -norm constraint, Eq. (1) can be reformulated as,

$$\min_{\mathbf{c}} \quad \|\mathbf{y} - \mathbf{X}\mathbf{c}\|_2^2 + \lambda \|\mathbf{c}\|_2^2, \quad \text{s.t. } \mathbf{c} \geq 0, \mathbf{1}^T \mathbf{c} = 1 \quad (2)$$

The above equation is the objective function of the proposed ANCR method.

B. Optimization

We adopt an alternative optimization strategy to solve the ANCR problem. By introducing an auxiliary variable \mathbf{z} , Eq. (2) can be rewritten as,

$$\min_{\mathbf{c}, \mathbf{z}} \quad \|\mathbf{y} - \mathbf{X}\mathbf{c}\|_2^2 + \lambda \|\mathbf{c}\|_2^2, \quad \text{s.t. } \mathbf{z} = \mathbf{c}, \mathbf{z} \geq 0, \mathbf{1}^T \mathbf{z} = 1 \quad (3)$$

The above optimization problem can be solved using the ADMM [19] method. Specifically, the Lagrangian function of Eq. (3) is,

$$\begin{aligned} \mathcal{L}(\mathbf{c}, \mathbf{z}, \delta, \rho) = & \|\mathbf{y} - \mathbf{X}\mathbf{c}\|_2^2 + \lambda \|\mathbf{c}\|_2^2 + \langle \delta, \mathbf{z} - \mathbf{c} \rangle \\ & + \frac{\rho}{2} \|\mathbf{z} - \mathbf{c}\|_2^2, \end{aligned} \quad (4)$$

where δ is the Lagrange multiplier and $\rho > 0$ is a penalty parameter. The optimization of Eq. (4) can be solved iteratively by updating \mathbf{c} and \mathbf{z} one at a time. The detailed updating procedures are presented as follows.

Update c: Fix the other variables and update \mathbf{c} by solving the following problem,

$$\min_{\mathbf{c}} \quad \|\mathbf{y} - \mathbf{X}\mathbf{c}\|_2^2 + \lambda \|\mathbf{c}\|_2^2 + \langle \delta, \mathbf{z} - \mathbf{c} \rangle + \frac{\rho}{2} \|\mathbf{z} - \mathbf{c}\|_2^2 \quad (5)$$

Algorithm 1 Solve Eq. (2) via ADMM

Input: Test sample \mathbf{y} , training data matrix \mathbf{X} , balancing parameter λ , $\text{tol} > 0$, $\rho > 0$ and the maximum iteration number T .

- 1: Initialize $\mathbf{z}_0 = \mathbf{c}_0 = \delta_0 = \mathbf{0}$;
- 2: **while** not converged **do**
- 3: Update \mathbf{c} by Eq. (6);
- 4: Update \mathbf{z} by solving Eq. (7);
- 5: Update δ by Eq. (8);
- 6: **end while**

Output: Coding vectors \mathbf{z} and \mathbf{c} .

Algorithm 2 Our proposed ANCR algorithm

Input: Training data matrix $\mathbf{X} = [\mathbf{X}_1, \mathbf{X}_2, \dots, \mathbf{X}_K] \in \mathbb{R}^{d \times n}$, test data $\mathbf{y} \in \mathbb{R}^d$ and balancing parameter λ .

- 1: Normalize the columns of \mathbf{X} and \mathbf{y} to have unit ℓ_2 norm;
- 2: Obtain the coding vector \mathbf{c} of \mathbf{y} on \mathbf{X} by solving the ANCR model in Eq. (2);
- 3: Compute the class-specific residuals $\mathbf{r}_i = \|\mathbf{y} - \mathbf{X}_i \mathbf{c}_i\|_2$;

Output: $\text{label}(\mathbf{y}) = \arg \min_i (\mathbf{r}_i)$

Setting the partial derivative of Eq. (5) with respect to \mathbf{c} to zero, we can obtain the following closed-form solution of \mathbf{c} ,

$$\mathbf{c}_{t+1} = [\mathbf{X}^T \mathbf{X} + \frac{(\rho + 2\lambda)}{2} \mathbf{I}]^{-1} [\mathbf{X}^T \mathbf{y} + \frac{\rho \mathbf{z}_t + \delta_t}{2}] \quad (6)$$

Update z: To update \mathbf{z} , we fix other variables and solve the following problem,

$$\min_{\mathbf{z}} \quad \left\| \mathbf{z} - \left(\mathbf{c} - \frac{\delta}{\rho} \right) \right\|_2^2, \quad \text{s.t. } \mathbf{z} \geq 0, \mathbf{1}^T \mathbf{z} = 1 \quad (7)$$

The above problem can be solved by the algorithm proposed by Huang *et al.* [38].

Update δ : The Lagrange multiplier δ is updated as

$$\delta_{t+1} = \delta_t + \rho(\mathbf{z}_{t+1} - \mathbf{c}_{t+1}) \quad (8)$$

The above procedures for solving Eq. (2) are summarized in Algorithm 1.

C. Classification

Given a test sample $\mathbf{y} \in \mathbb{R}^d$, we first obtain its coding vector \mathbf{c} over the entire training data \mathbf{X} by Algorithm 1. Then the test sample is assigned into the class that yields the least residual, i.e., $\text{identity}(\mathbf{y}) = \arg \min_i \|\mathbf{y} - \mathbf{X}_i \mathbf{c}_i\|_2$, where \mathbf{c}_i is the coding vector that belongs to the i -th class. The complete process of the proposed ANCR method is summarized in Algorithm 2.

IV. EXPERIMENTS AND ANALYSIS

In this section, we evaluate the classification performance of ANCR on several benchmarking datasets, including the AR database [39] for face recognition, USPS dataset [40] for handwritten digit classification, Stanford 40 Actions

TABLE I
A COMPARISON OF THE PROPOSED METHOD IN TERMS OF RECOGNITION ACCURACY (%) ON THE AR DATABASE.

Dimensions	54	120	300
NSC [45]	70.7	75.5	76.1
SVM	81.6	89.3	91.6
SRC [1]	82.1	88.3	90.3
CRC [2]	80.3	90.1	93.8
CROC [46]	82.0	90.8	93.7
ProCRC [47]	81.4	90.7	93.7
SA-CRC [7]	75.1	86.7	92.5
CCRC [48]	81.2	88.9	93.1
NRC [17]	85.2	91.3	93.3
ANCR	86.0	91.3	94.0

dataset [41] for action recognition, three fine-grained object datasets which includes the CUB-200-2011 dataset [42], the Aircraft dataset [43] and the Cars dataset [44]. We compare the classification accuracy of ANCR with NSC [45], linear SVM, SRC [1], CRC [2], CROC [46], ProCRC [47], SA-CRC [7], CCRC [48] and NRC [17]. In addition, on the Aircraft and Cars datasets, we also compare ANCR with key deep methods, such as VGG19 [49], FV-FGC [50], and B-CNN [51].

A. Experiments on the AR Database

The AR database [39] comprises over 4000 frontal images for 126 individuals, these images contain variations in facial expressions, illumination and occlusions. Following the experimental settings in [17], in our experiments, we use the subset with only illumination and expression changes. This subset contains 50 male and 50 female subjects. For each subject, 7 images from Session 1 are used as training samples, and 7 images from Session 2 are used as test samples. All the images are cropped to 60×43 pixels and projected to a subspace of dimensions 54, 120, and 300 by PCA. The experimental results are listed in Table I. Note, the balancing parameter λ of ANCR is set to $1e-4$. We can observe that our proposed ANCR consistently outperforms the other methods under all the three reduced dimensions.

B. Experiments on the USPS Dataset

The USPS dataset [40] consists of 9298 images of digit numbers, i.e. from 0 to 9. The training set and test set of USPS have 7291 and 2007 images, respectively. All the images are resized into 16×16 pixels. For each class, N ($N=50, 100, 200, 300$) images from the training set are randomly selected for training and all the images in the test set are used for testing. Experiments are repeated for 10 times and the average results are reported in Table II. The balancing parameter λ of ANCR is set to 0.001. We can see that ANCR achieves the best recognition result for all the settings. With the increase of the number of training images, the recognition accuracy of all the approaches improves steadily.

TABLE II
A COMPARISON OF THE PROPOSED METHOD IN TERMS OF RECOGNITION ACCURACY (%) ON THE USPS DATASET.

N	50	100	200	300
NSC [45]	91.2	92.2	92.8	92.8
SVM	91.6	92.5	93.1	93.2
SRC [1]	89.1	91.2	92.9	93.8
CRC [2]	89.8	90.8	91.5	91.5
CROC [46]	91.9	91.3	91.7	91.8
ProCRC [47]	90.9	91.9	92.2	92.2
SA-CRC [7]	86.4	88.5	90.5	91.3
CCRC [48]	90.9	92.2	93.1	93.0
NRC [17]	90.3	91.6	92.7	93.0
ANCR	92.1	93.0	93.5	94.3



Fig. 2. Example images from the Stanford 40 Actions dataset.

TABLE III
A COMPARISON OF THE PROPOSED METHOD IN TERMS OF RECOGNITION ACCURACY (%) ON THE STANFORD 40 ACTIONS DATASET.

Methods	Accuracy	Methods	Accuracy
Softmax	77.2	CCRC [48]	79.2
NSC [45]	74.7	NRC [17]	81.1
SRC [1]	78.7	AlexNet [52]	68.6
CRC [2]	78.2	EPM [53]	72.3
CROC [46]	79.2	ASPD [54]	75.4
ProCRC [47]	80.9	VGG19 [49]	77.2
SA-CRC [7]	77.3	ANCR	81.3

C. Experiments on the Stanford 40 Actions Dataset

The Stanford 40 Actions dataset [41] has 40 different classes of human actions, e.g., applauding, blowing bubbles, and cooking. Some example images from the dataset are shown in Fig. 2. This dataset contains 9352 images in total, 180 to 300 images per action. Following the training-test split settings scheme in [17], we randomly select 100 images per class as the training images and use the remaining images as the test set. The balancing parameter λ of ANCR is set to 0.001. We extract image features by the pre-trained VGG-19 network. The dimensionality of the extracted VGG feature vector of each image is 4096. AlexNet [52], EPM [53], ASPD [54] and VGG-19 [49] are used for comparison. EPM and ASPD are two leading approaches for action recognition with still images. Experimental results are reported in Table III. One can see that ANCR outperforms both the conventional representation based classification methods and the deep learning models in terms of recognition accuracy, which again validates the superiority of the proposed method.



Fig. 3. Example images from the CUB-200-2011 dataset.

TABLE IV

A COMPARISON OF THE PROPOSED METHOD IN TERMS OF RECOGNITION ACCURACY (%) ON THE CUB-200-2011 DATASET.

Methods	Accuracy	Methods	Accuracy
Softmax	72.1	CCRC [48]	75.4
NSC [45]	74.5	NRC [17]	78.3
SRC [1]	76.0	POOF [55]	56.9
CRC [2]	76.2	FV-CNN [56]	66.7
CROC [46]	76.2	VGG19 [49]	71.9
ProCRC [47]	78.3	PN-CNN [57]	75.7
SA-CRC [7]	75.5	ANCR	78.6

D. Experiments on the CUB-200-2011 Dataset

The Caltech-UCSD Birds 200 (CUB-200-2011) [42] is a representative fine-grained object classification dataset with images of 200 bird categories, there are 11,788 images and each category has about 60 images. This dataset is an extended version of the CUB-200 dataset. Some example images of the dataset are shown in Fig. 3. We use the publicly available split [42], which uses nearly half of the images in this dataset as the training samples and the other half as the test samples. Features are extracted by using the pre-trained VGG-19 network and the balancing parameter λ of ANCR is set to 0.001. POOF [55], FV-CNN [56], VGG-19 [49] and PN-CNN [57] are also included for comparison. Experimental results are shown in Table IV. According to the table, we can see that ANCR achieves the best recognition accuracy on the CUB-200-2011 dataset.

E. Experiments on the Aircraft Dataset

The Aircraft dataset [43] contains 10,000 images of 100 different aircraft model variants, example images of this dataset are shown in Fig. 4. Following the experimental settings in [17], 6667 images are used for training and 3333 images for testing. The image features are extracted by the pre-trained VGG-16 network. The balancing parameter λ of ANCR is set to 0.001. We also compare our method with VGG-16 [49], Symbiotic [58], FV-FGC [50] and B-CNN [51]. The recognition accuracy of each approach is presented in Table V. Again, our proposed ANCR method outperforms all the other approaches.

F. Experiments on the Cars Dataset

The Cars dataset [44] contains 16,185 images of 196 classes of cars, some example images of this dataset are shown in Fig. 5. Following the standard evaluation protocol [44], 8144



Fig. 4. Example images from Aircraft dataset.

TABLE V

A COMPARISON OF THE PROPOSED METHOD IN TERMS OF RECOGNITION ACCURACY (%) ON THE AIRCRAFT DATASET.

Methods	Accuracy	Methods	Accuracy
Softmax	85.6	CCRC [48]	87.5
NSC [45]	85.5	NRC [17]	87.3
SRC [1]	86.1	VGG16 [49]	85.6
CRC [2]	86.7	Symbiotic [58]	72.5
CROC [46]	86.9	FV-FGC [50]	80.7
ProCRC [47]	86.8	B-CNN [51]	84.1
SA-CRC [7]	86.9	ANCR	87.7

TABLE VI

A COMPARISON OF THE PROPOSED METHOD IN TERMS OF RECOGNITION ACCURACY (%) ON THE CARS DATASET.

Methods	Accuracy	Methods	Accuracy
Softmax	88.7	CCRC [48]	90.6
NSC [45]	88.3	NRC [17]	90.7
SRC [1]	89.2	VGG16 [49]	88.7
CRC [2]	90.0	Symbiotic [58]	78.0
CROC [46]	90.3	FV-FGC [50]	82.7
ProCRC [47]	90.1	B-CNN [51]	90.6
SA-CRC [7]	90.4	ANCR	90.7

images are used for training and the other 8041 images are used for testing. Image features are extracted via a pre-trained VGG-16 network. The balancing parameter λ of ANCR is set to 0.001. As on the Aircraft dataset, we compare the proposed method with VGG-16 [49], Symbiotic [58], FV-FGC [50] and B-CNN [51] on this dataset. The results are reported in terms of accuracy in Table VI. It can be seen that our proposed ANCR method achieves comparable performance as NRC, and it is superior to the other methods.



Fig. 5. Example images from the Cars dataset.

G. Ablation Study

In this subsection, we demonstrate the effectiveness of the non-negative constraint and affine constraint in ANCR by

conducting ablation studies. To explore the impact of each constraint, we compare ANCR with several baseline models.

By discarding both the non-negative and affine constraints in Eq. (2), we can obtain the first baseline model,

$$\min_{\mathbf{c}} \|\mathbf{y} - \mathbf{X}\mathbf{c}\|_2^2 + \lambda \|\mathbf{c}\|_2^2, \quad (9)$$

which actually is the objective function of CRC, and Eq. (9) has the following closed-form solution,

$$\mathbf{c} = (\mathbf{X}^T \mathbf{X} + \lambda \mathbf{I})^{-1} \mathbf{X}^T \mathbf{y}. \quad (10)$$

When removing the non-negative constraint from Eq. (2), we obtain the following problem,

$$\min_{\mathbf{c}} \|\mathbf{y} - \mathbf{X}\mathbf{c}\|_2^2 + \lambda \|\mathbf{c}\|_2^2, \text{ s.t. } \mathbf{1}^T \mathbf{c} = 1, \quad (11)$$

which can be called the affine collaborative representation (ACR) model. By algebraic manipulations, one can derive the following closed-form solution to ACR,

$$\mathbf{c} = \hat{\mathbf{c}} / \mathbf{1}^T \hat{\mathbf{c}}, \quad \hat{\mathbf{c}} = (\mathbf{M} + \lambda \mathbf{I})^{-1} \mathbf{1}, \quad (12)$$

where $\mathbf{M} = (\mathbf{X}^T - \mathbf{1}\mathbf{y}^T)(\mathbf{X}^T - \mathbf{1}\mathbf{y}^T)^T$.

By omitting the affine constraint in Eq. (2), we get the following problem,

$$\min_{\mathbf{c}} \|\mathbf{y} - \mathbf{X}\mathbf{c}\|_2^2 + \lambda \|\mathbf{c}\|_2^2, \text{ s.t. } \mathbf{c} \geq 0, \quad (13)$$

which is termed as the non-negative collaborative representation (NCR) model. Similar to the proposed ANCR method, NCR can be solved by the ADMM algorithm [19].

ANCR and the above three baseline models are summarized in Table VII. Experiments are conducted on the six datasets and the experimental results are reported in Tables VIII-X, respectively. Based on the experimental results, the following observations can be made.

(1) NCR outperforms CRC in most cases, which indicates that the coding vector obtained by NCR contains more discriminative information than that of CRC, thus enhancing the classification capability of CRC.

(2) ACR is inferior to CRC except on the Aircraft and Cars datasets, which shows that by introducing just the affine constraint into the framework of CRC, the solution cannot guarantee that the classification accuracy be consistently improved.

(3) Our proposed ANCR method performs better in recognition accuracy than the other three baseline models. This demonstrates the role of both, the non-negative regularization and the affine constraint in our ANCR method.

H. Convergence and Parameter Sensitiveness Analysis

The convergence of ADMM with two variable has been proven by Boyd *et al.* [19]. Here we present the convergence curves on the six datasets in Fig. 6. We can see that the objective function value of ANCR gradually decreases with the increasing number of iterations, which empirically demonstrates the convergence of the proposed ANCR approach.

To examine how the balancing parameter λ influences the performance of ANCR, we conducted experiments on the four

TABLE VII
SUMMARY OF OUR ANCR AND THE THREE BASELINE MODELS CRC, ACR AND NCR.

Models	Regularization terms	Constraints	
		$\mathbf{c} \geq 0$	$\mathbf{1}^T \mathbf{c} = 1$
CRC [2]	$\ \mathbf{y} - \mathbf{X}\mathbf{c}\ _2^2 + \lambda \ \mathbf{c}\ _2^2$	\times	\times
ACR		\times	\checkmark
NCR		\checkmark	\times
ANCR		\checkmark	\checkmark

TABLE VIII
RECOGNITION ACCURACY (%) OF CRC, ACR, NCR AND ANCR ON THE AR DATABASE.

Dimensions	54	120	300
CRC [2]	80.3	90.1	93.8
ACR	78.5	88.5	91.4
NCR	85.2	91.3	93.3
ANCR	86.0	91.3	94.0

TABLE IX
RECOGNITION ACCURACY (%) OF CRC, ACR, NCR AND ANCR ON THE USPS DATASET.

N	50	100	200	300
CRC [2]	89.8	90.8	91.5	91.5
ACR	85.6	87.9	89.3	89.5
NCR	90.2	91.6	92.6	92.9
ANCR	92.1	93.0	93.5	94.3

TABLE X
RECOGNITION ACCURACY (%) OF CRC, ACR, NCR AND ANCR ON THE FOUR LARGE SCALE DATASETS.

Methods	Stanford 40	CUB-200-2011	Aircraft	Cars
CRC [2]	78.2	76.2	86.7	90.0
ACR	66.8	70.4	87.4	90.5
NCR	81.1	78.4	87.3	90.6
ANCR	81.3	78.6	87.7	90.7

large-scale datasets. The experimental settings are the same as those described in the above sub-sections. Fig. 7 plots the recognition accuracy with varying λ . We can see that ANCR returns stable results for a wide range of λ values, i.e., $[0.0001, 0.01]$. When λ increases from 0.01 to 0.1, the performance of ANCR drops a little. Larger value of λ means that ANCR will emphasize the ℓ_2 -norm of the coding vector, which could undermine the collaborative mechanism of all the training samples in representing a test sample. Therefore, we set a relatively small value for λ in our experiments.

V. CONCLUSION

To further enhance the classification performance of NRC, in this paper, we developed an affine non-negative collaborative representation (ANCR) model. ANCR is derived by introducing a regularizer on the coding vector, as well as an affine constraint into the formulation of NRC. Our proposed

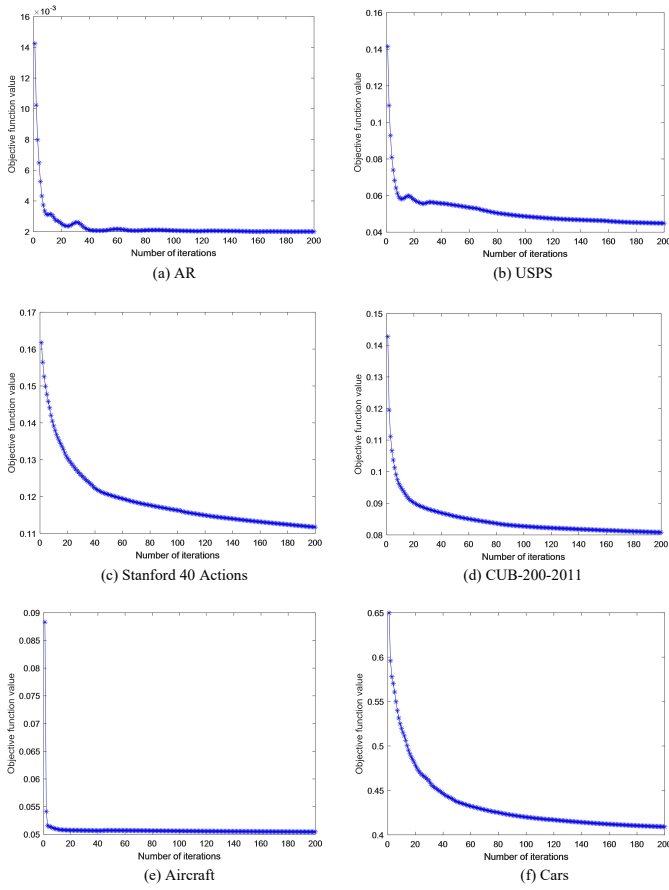


Fig. 6. Convergence curves of ANCR on different datasets: (a)-(f) are the convergence curves obtained in the experiments performed on the AR, USPS, Stanford 40 Actions, CUB-200-2011, Aircraft and Cars datasets, respectively.

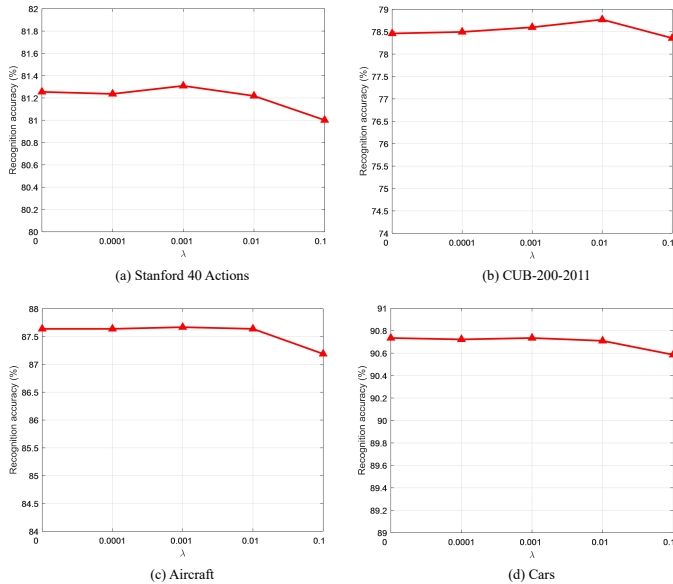


Fig. 7. Recognition accuracy (%) of ANCR with varying parameter λ on (a) Stanford 40 Actions (b) CUB-200-2011 (c) Aircraft and (d) Cars datasets, respectively.

ANCR method is solved elegantly by ADMM. The experimental results on six well-known datasets demonstrate the superiority of the proposed ANCR method over NRC and traditional representation based classification methods. The proposed method also outperforms some deep learning based approaches.

ACKNOWLEDGMENTS

The work was supported in part by the National Natural Science Foundation of China (61672265, U1836218, 61902153), in part by the 111 Project of the Ministry of Education of China (B12018), in part by the EPSRC programme grant (EP/N007743/1) and in part by the EPSRC/dstl/MURI project (EP/R018456/1).

REFERENCES

- [1] J. Wright, A. Y. Yang, A. Ganesh, S. Sastry, and Y. Ma, "Robust face recognition via sparse representation," *IEEE Transactions on Pattern Analysis and Machine Intelligence*, vol. 31, no. 2, pp. 210–227, 2009.
- [2] L. Zhang, M. Yang, and X. Feng, "Sparse representation or collaborative representation: Which helps face recognition?" in *2011 International Conference on Computer Vision*. IEEE, 2011, pp. 471–478.
- [3] Q. Liu and C. Liu, "A novel locally linear knn method with applications to visual recognition," *IEEE Transactions on Neural Networks and Learning Systems*, vol. 28, no. 9, pp. 2010–2021, 2016.
- [4] X. Song, Z.-H. Feng, G. Hu, X. Yang, J.-y. Yang, and Y. Qi, "Progressive sparse representation-based classification using local discrete cosine transform evaluation for image recognition," *Journal of Electronic Imaging*, vol. 24, no. 5, p. 053010, 2015.
- [5] J. Lai and X. Jiang, "Classwise sparse and collaborative patch representation for face recognition," *IEEE Transactions on Image Processing*, vol. 25, no. 7, pp. 3261–3272, 2016.
- [6] C. Shao, X. Song, Z.-H. Feng, X.-J. Wu, and Y. Zheng, "Dynamic dictionary optimization for sparse-representation-based face classification using local difference images," *Information Sciences*, vol. 393, pp. 1–14, 2017.
- [7] N. Akhtar, F. Shafait, and A. Mian, "Efficient classification with sparsity augmented collaborative representation," *Pattern Recognition*, vol. 65, pp. 136–145, 2017.
- [8] Z.-Q. Li, J. Sun, X.-J. Wu, and H.-F. Yin, "Sparsity augmented weighted collaborative representation for image classification," *Journal of Electronic Imaging*, vol. 28, no. 5, p. 053032, 2019.
- [9] W. Deng, J. Hu, and J. Guo, "Face recognition via collaborative representation: Its discriminant nature and superposed representation," *IEEE Transactions on Pattern Analysis and Machine Intelligence*, vol. 40, no. 10, pp. 2513–2521, 2018.
- [10] D. M. Vo and S.-W. Lee, "Robust face recognition via hierarchical collaborative representation," *Information Sciences*, vol. 432, pp. 332–346, 2018.
- [11] X. Song, Z.-H. Feng, G. Hu, J. Kittler, and X.-J. Wu, "Dictionary integration using 3d morphable face models for pose-invariant collaborative-representation-based classification," *IEEE Transactions on Information Forensics and Security*, vol. 13, no. 11, pp. 2734–2745, 2018.
- [12] C. Zheng and N. Wang, "Collaborative representation with k-nearest classes for classification," *Pattern Recognition Letters*, vol. 117, pp. 30–36, 2019.
- [13] W.-Y. Xie, B.-D. Liu, S. Shao, Y. Li, and Y.-J. Wang, "Sparse representation and collaborative representation? both help image classification," *IEEE Access*, vol. 7, pp. 76 061–76 070, 2019.
- [14] X. Song, Z.-H. Feng, G. Hu, and X.-J. Wu, "Half-face dictionary integration for representation-based classification," *IEEE Transactions on Cybernetics*, vol. 47, no. 1, pp. 142–152, 2017.
- [15] R. Lan, Y. Zhou, Z. Liu, and X. Luo, "Prior knowledge-based probabilistic collaborative representation for visual recognition," *IEEE Transactions on Cybernetics*, vol. 50, no. 4, pp. 1498–1508, 2020.
- [16] J. Gou, L. Wang, Z. Yi, Y. Yuan, W. Ou, and Q. Mao, "Weighted discriminative collaborative competitive representation for robust image classification," *Neural Networks*, vol. 125, pp. 104–120, 2020.

- [17] J. Xu, W. An, L. Zhang, and D. Zhang, "Sparse, collaborative, or nonnegative representation: Which helps pattern classification?" *Pattern Recognition*, vol. 88, pp. 679–688, 2019.
- [18] D. D. Lee and H. S. Seung, "Learning the parts of objects by non-negative matrix factorization," *Nature*, vol. 401, no. 6755, pp. 788–791, 1999.
- [19] S. Boyd, N. Parikh, and E. Chu, *Distributed optimization and statistical learning via the alternating direction method of multipliers*. Now Publishers Inc, 2011.
- [20] N. Vo, B. Moran, and S. Challa, "Nonnegative-least-square classifier for face recognition," in *International Symposium on Neural Networks*. Springer, 2009, pp. 449–456.
- [21] L. Zhuang, H. Gao, Z. Lin, Y. Ma, X. Zhang, and N. Yu, "Non-negative low rank and sparse graph for semi-supervised learning," in *2012 IEEE Conference on Computer Vision and Pattern Recognition*. IEEE, 2012, pp. 2328–2335.
- [22] M. Yin, J. Gao, and Z. Lin, "Laplacian regularized low-rank representation and its applications," *IEEE Transactions on Pattern Analysis and Machine Intelligence*, vol. 38, no. 3, pp. 504–517, 2015.
- [23] T. Xu, X.-J. Wu, and J. Kittler, "Non-negative subspace representation learning scheme for correlation filter based tracking," in *2018 24th International Conference on Pattern Recognition (ICPR)*. IEEE, 2018, pp. 1888–1893.
- [24] S. Zhang, J. Wang, W. Shi, Y. Gong, Y. Xia, and Y. Zhang, "Normalized non-negative sparse encoder for fast image representation," *IEEE Transactions on Circuits and Systems for Video Technology*, vol. 29, no. 7, pp. 1962–1972, 2018.
- [25] Z. Chen, X.-J. Wu, and J. Kittler, "Non-negative representation based discriminative dictionary learning for face recognition," in *International Conference on Image and Graphics*. Springer, 2019, pp. 307–319.
- [26] J. Xu, M. Yu, L. Shao, W. Zuo, D. Meng, L. Zhang, and D. Zhang, "Scaled simplex representation for subspace clustering," *IEEE Transactions on Cybernetics*, 2019.
- [27] J. Xu, Z. Xu, W. An, H. Wang, and D. Zhang, "Non-negative sparse and collaborative representation for pattern classification," *arXiv preprint arXiv:1908.07956*, 2019.
- [28] Y.-P. Zhao, L. Chen, and C. P. Chen, "Laplacian regularized nonnegative representation for clustering and dimensionality reduction," *IEEE Transactions on Circuits and Systems for Video Technology*, 2020.
- [29] H.-F. Yin and X.-J. Wu, "Class-specific residual constraint non-negative representation for pattern classification," *Journal of Electronic Imaging*, vol. 29, no. 2, p. 023014, 2020.
- [30] E. Elhamifar and R. Vidal, "Sparse subspace clustering," in *2009 IEEE Conference on Computer Vision and Pattern Recognition*. IEEE, 2009, pp. 2790–2797.
- [31] —, "Sparse subspace clustering: Algorithm, theory, and applications," *IEEE Transactions on Pattern Analysis and Machine Intelligence*, vol. 35, no. 11, pp. 2765–2781, 2013.
- [32] Y. Xu and X. Wu, "An affine subspace clustering algorithm based on ridge regression," *Pattern Analysis and Applications*, vol. 20, no. 2, pp. 557–566, 2017.
- [33] W. Dong and X. Wu, "Robust affine subspace clustering via smoothed ℓ_0 -norm," *Neural Processing Letters*, vol. 50, no. 1, pp. 785–797, 2019.
- [34] J. Wang, J. Yang, K. Yu, F. Lv, T. Huang, and Y. Gong, "Locality-constrained linear coding for image classification," in *2010 IEEE Conference on Computer Vision and Pattern Recognition*. IEEE, 2010, pp. 3360–3367.
- [35] C.-P. Wei, Y.-W. Chao, Y.-R. Yeh, and Y.-C. F. Wang, "Locality-sensitive dictionary learning for sparse representation based classification," *Pattern Recognition*, vol. 46, no. 5, pp. 1277–1287, 2013.
- [36] B.-B. Benuwa, B. Ghansah, and E. K. Ansah, "Kernel based locality-sensitive discriminative sparse representation for face recognition," *Scientific African*, vol. 7, p. e00249, 2020.
- [37] H. Zou and T. Hastie, "Regularization and variable selection via the elastic net," *Journal of the royal statistical society: series B (statistical methodology)*, vol. 67, no. 2, pp. 301–320, 2005.
- [38] J. Huang, F. Nie, and H. Huang, "A new simplex sparse learning model to measure data similarity for clustering," in *Twenty-Fourth International Joint Conference on Artificial Intelligence*, 2015.
- [39] A. M. Martinez, "The ar face database," *CVC Technical Report24*, 1998.
- [40] J. J. Hull, "A database for handwritten text recognition research," *IEEE Transactions on Pattern Analysis and Machine Intelligence*, vol. 16, no. 5, pp. 550–554, 1994.
- [41] B. Yao, X. Jiang, A. Khosla, A. L. Lin, L. Guibas, and L. Fei-Fei, "Human action recognition by learning bases of action attributes and parts," in *2011 International Conference on Computer Vision*. IEEE, 2011, pp. 1331–1338.
- [42] C. Wah, S. Branson, P. Welinder, P. Perona, and S. Belongie, "The Caltech-UCSD Birds-200-2011 Dataset," California Institute of Technology, Tech. Rep. CNS-TR-2011-001, 2011.
- [43] S. Maji, E. Rahtu, J. Kannala, M. Blaschko, and A. Vedaldi, "Fine-grained visual classification of aircraft," *arXiv preprint arXiv:1306.5151*, 2013.
- [44] J. Krause, M. Stark, J. Deng, and F.-F. Li, "3d object representations for fine-grained categorization," in *Proceedings of the IEEE International Conference on Computer Vision Workshops*, 2013, pp. 554–561.
- [45] K. Lee, J. Ho, and D. J. Kriegman, "Acquiring linear subspaces for face recognition under variable lighting," *IEEE Transactions on Pattern Analysis and Machine Intelligence*, vol. 27, no. 5, pp. 684–698, 2005.
- [46] Y. Chi and F. Porikli, "Classification and boosting with multiple collaborative representations," *IEEE Transactions on Pattern Analysis and Machine Intelligence*, vol. 36, no. 8, pp. 1519–1531, 2014.
- [47] S. Cai, L. Zhang, W. Zuo, and X. Feng, "A probabilistic collaborative representation based approach for pattern classification," in *Proceedings of the IEEE Conference on Computer Vision and Pattern Recognition*, 2016, pp. 2950–2959.
- [48] H. Yuan, X. Li, F. Xu, Y. Wang, L. L. Lai, and Y. Y. Tang, "A collaborative-competitive representation based classifier model," *Neurocomputing*, vol. 275, pp. 627–635, 2018.
- [49] K. Simonyan and A. Zisserman, "Very deep convolutional networks for large-scale image recognition," pp. 1–14, 2015.
- [50] P.-H. Gosselin, N. Murray, H. Jégou, and F. Perronnin, "Revisiting the fisher vector for fine-grained classification," *Pattern Recognition Letters*, vol. 49, pp. 92–98, 2014.
- [51] T.-Y. Lin, A. RoyChowdhury, and S. Maji, "Bilinear cnn models for fine-grained visual recognition," in *Proceedings of the IEEE International Conference on Computer Vision*, 2015, pp. 1449–1457.
- [52] A. Krizhevsky, I. Sutskever, and G. E. Hinton, "Imagenet classification with deep convolutional neural networks," in *Advances in Neural Information Processing Systems*, 2012, pp. 1097–1105.
- [53] G. Sharma, F. Jurie, and C. Schmid, "Expanded parts model for human attribute and action recognition in still images," in *Proceedings of the IEEE Conference on Computer Vision and Pattern Recognition*, 2013, pp. 652–659.
- [54] F. S. Khan, J. Xu, J. Van De Weijer, A. D. Bagdanov, R. M. Anwer, and A. M. Lopez, "Recognizing actions through action-specific person detection," *IEEE Transactions on Image Processing*, vol. 24, no. 11, pp. 4422–4432, 2015.
- [55] T. Berg and P. Belhumeur, "Poof: Part-based one-vs.-one features for fine-grained categorization, face verification, and attribute estimation," in *Proceedings of the IEEE Conference on Computer Vision and Pattern Recognition*, 2013, pp. 955–962.
- [56] M. Cimpoi, S. Maji, and A. Vedaldi, "Deep filter banks for texture recognition and segmentation," in *Proceedings of the IEEE Conference on Computer Vision and Pattern Recognition*, 2015, pp. 3828–3836.
- [57] S. Branson, G. Van Horn, S. Belongie, and P. Perona, "Bird species categorization using pose normalized deep convolutional nets," 2014.
- [58] Y. Chai, V. Lempitsky, and A. Zisserman, "Symbiotic segmentation and part localization for fine-grained categorization," in *Proceedings of the IEEE International Conference on Computer Vision*, 2013, pp. 321–328.